Analyzing the atmosphere of an exoplanet

Candidate 15342, Candidate 15341
(Dated: December 5, 2022)

In this paper we analyze the atmosphere of an unknown planet. First we will look into how one would get into close orbit by decelerating the right amount at the tight time. From the low orbit we were able to take pictures of the planets surface and through these determined a suitable landing site. Next we will look at how to analyze the absorption spectre coming from the atmosphere. We use the method of χ^2-minimization and an algorithm inspired by the Gibbs sampler method in order to find the best fitting line-profiles. Of the twelve absorption lines we looked for, we found four lines that are likely to be real. With the help of these we were able to model the atmospheres by creating profiles of the temperature, density and pressure. **We wish to only be evaluated on how we solved the challenge, results, conclusion and the discussion**

CONTENTS

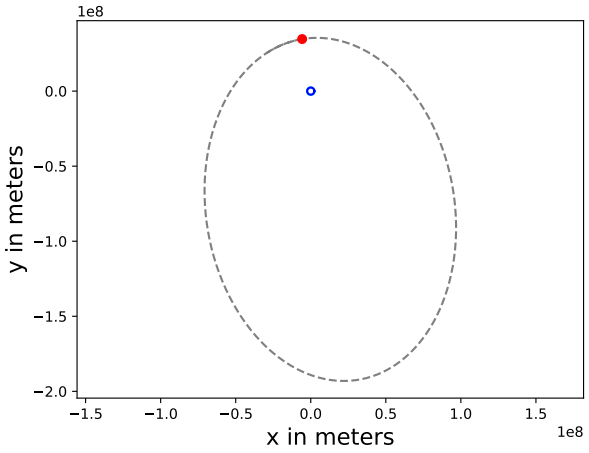

Figure 1. First orbit around planet (blue) before adjusting trajectory. Red dot marks ship position

increasing the distance to the planet, not falling into it because of drag from the atmosphere.

‘

I. RESULTS

A. Low orbit

Figures 1, 2 and 3 show the three stages of the maneuvers to get into low orbit. First is the orbit we have after the orbital injection maneuver. Second image is after boosting in retrograde close to the periapsis with 70% of the angular velocity in that point. Last figure is after a second retrograde boost of 26% of the angular velocity. The final orbit is near circular with an eccentricity of 0.01356. One orbit takes 8024 seconds, or 2.2 hours.

We did not enter the atmosphere, we know this as our distance to the planet remains between 2 898 km and 2 969 km from the centre. rather, it looks like we are

B. Possible landing sites

In low orbit we could take detailed pictures of the planets surface. Analyzing these, we scouted for optimal landing sites. The rocket orbited around the planet for 14000 seconds, taking a picture every 1000 seconds. As we had found that one orbit takes 8024 we got pictures from every angle of the planet. The orbit remained in the x-y-plane according to the planet. At the same time the picture of a potential landing site was taken, the position of it was marked. First we went around once and found possible landing sites. One area, between the angle of 0° to 64° seemed interesting. As we circled back around we saw 4 at $\phi = 23°$. We chose this as a optimal landing site.

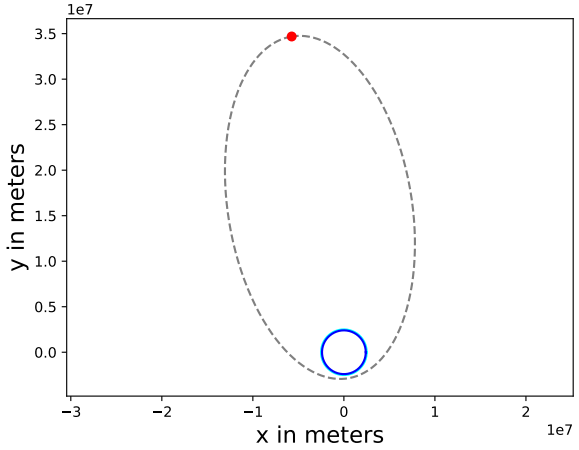

Figure 2. Orbit after first deceleration. Red dot marks ship, cyan circle marks 100 km over the surface where there could be an atmosphere, blue circle marks planet.

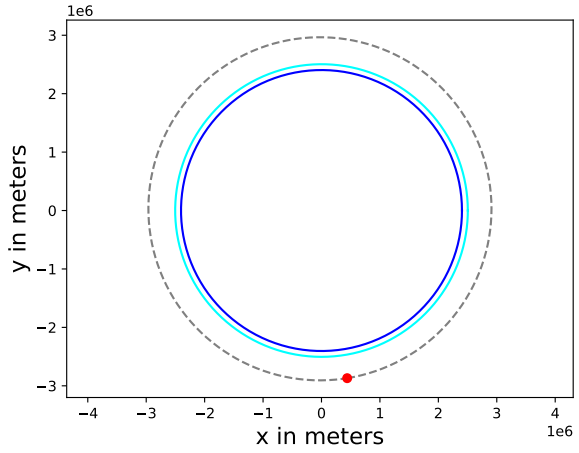

Figure 3. Final orbit after second deceleration. Red dot marks ship, cyan circle marks 100 km over the surface where there could be an atmosphere, blue circle marks planet.

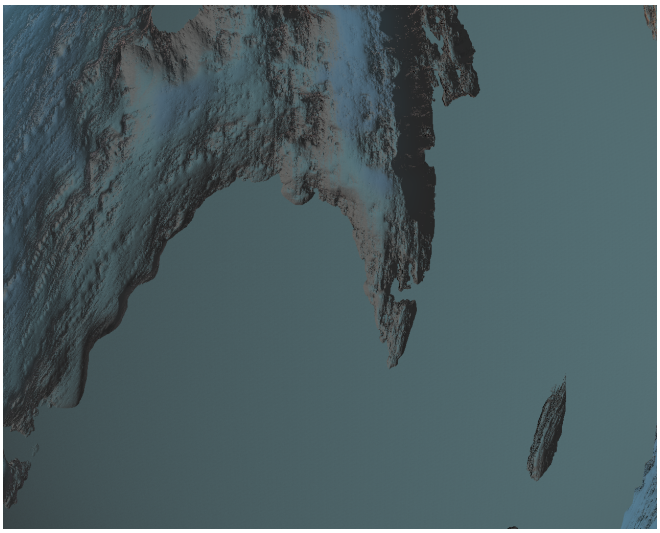

Figure 4. Picture of a potential landing site, taken at angle of $\phi = 23°$

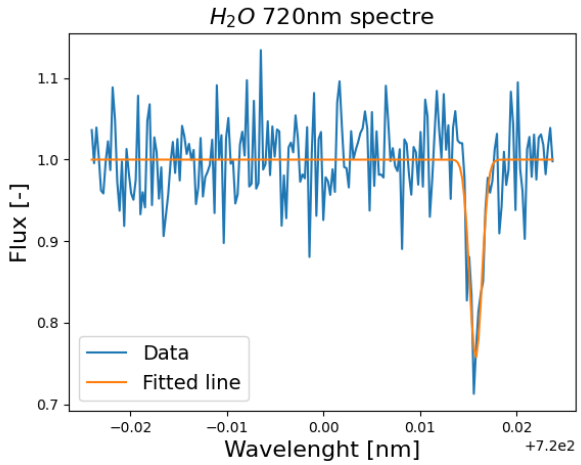

Figure 5. H_2O 720nm, the most confident result. Blue graph shows the data, while the orange line is the best fitting model.

C. Search for absorption lines

With as much noise as this data has, it is hard to decide which lines are real and which are flukes, however our best estimate is that the atmosphere is mainly composed of water vapor (H_2O). carbon monoxide (CO) and oxygen (O_2)

In the appendix you can find plots of the normalized data at different wavelengths compared to the best model our algorithm could find. The models we found to be reasonable are the models for spectral lines H_2O 720nm, H_2O 940nm, O_2 690nm and CO 2340nm. Remember to read the introductory text before the graphs in order to make sense of them.

We designed an algorithm in order to generate models of the line profile that fit the data. These helped to identify which lines were true absorption lines and which were not. In figure V B and 6 respectively you can see an example of a real absorption line and an obvious fluke. You can also see the algorithms best model for a line profile. The true detection has a clear and sudden fall in flux, while the fluke has no such defined shape.

In order to produce the models, we had algorithms to decide three parameters: The wavelength that the line profile is centered around, which differs from the laboratory wavelength because of the Doppler effect. The temperature of the gas, and the flux at the centre of the line profile. In table 1 we see all these parameters, where the first two columns, 'gas' and 'λ_0' are input data, and the last three are the results from the analysis.

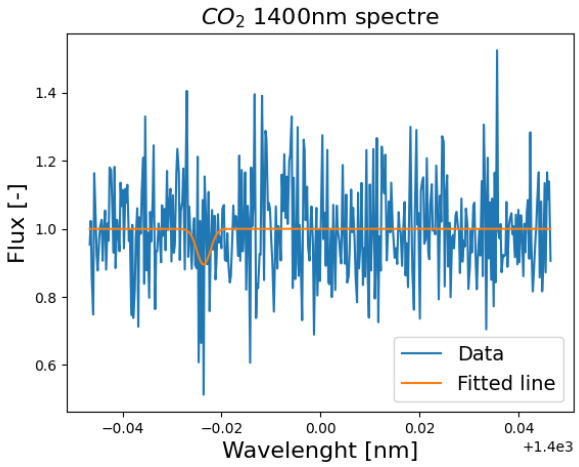

Figure 6. CO_2 1400nm, an example of a clear fluke. Blue graph shows the data, while the orange line is the best fitting model.

gas	λ_0 [nm]	λ [nm]	T [K]	F_{min}[-]
O_2	632	631.986	150	0.74
O_2	690	690.015	421	0.70
O_2	760	760.021	160	0.88
H_2O	720	720.016	156	0.76
H_2O	820	820.018	209	0.84
H_2O	940	940.021	152	0.71
CO_2	1400	1399.98	450	0.89
CO_2	1600	1600.04	150	0.82
CH_4	1660	1660.04	450	0.80
CH_4	2200	2200.05	393	0.89
CO	2340	2340.05	432	0.83
N_2O	2870	2870.06	241	0.83

D. Atmospheric profile

From our previous calculations we were able to numerically deduced the pressure, temperature and density to any distance above the planet surface. We model the atmosphere as adiabatic until the height where the temperature is half that of the surface temperature $290.7K$. The temperature reaches $145.35K$ at the height of about 61.65km above the surface. Afterwards the atmosphere is modelled as isothermal, with the constant temperature of 145.35K.

The numerical methods gave the temperature and density profile shown in figure 7 and 8 respectively. In figure 7 we see that the temperature starts at the surface temperature 290.7K. Then it declines linearly in the adiabatic atmosphere and per definition remains constant in the isothermal atmosphere. The switch between atmospheric types is represented by the grey dotted line.

In 8 we see how the density starts at the value of $1.802\frac{kg}{m^3}$ and exponentially declines, ending at the value of $3.59 \cdot 10^{-10}\frac{kg}{m^3}$. The transition from adiabetic to isothermal makes the density decline somewhat steeper, yet still exponential. The density nears zero at very high altitudes.

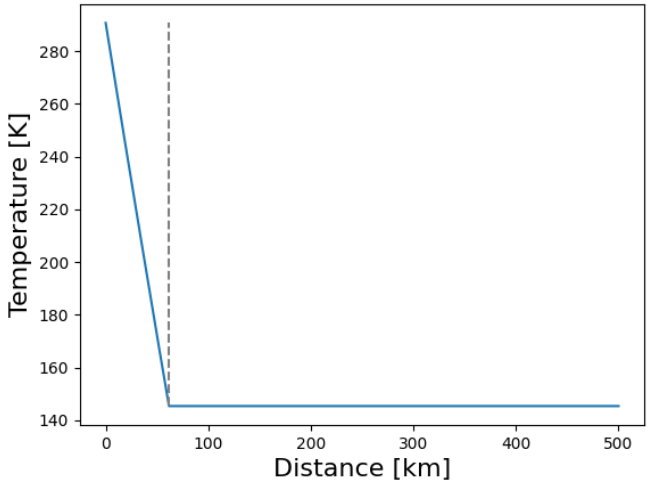

Figure 7. Temperature from surface to 80 km above surface. The dotted line is the border between the adiabatic and isothermal atmosphere at about 500km above the surface.

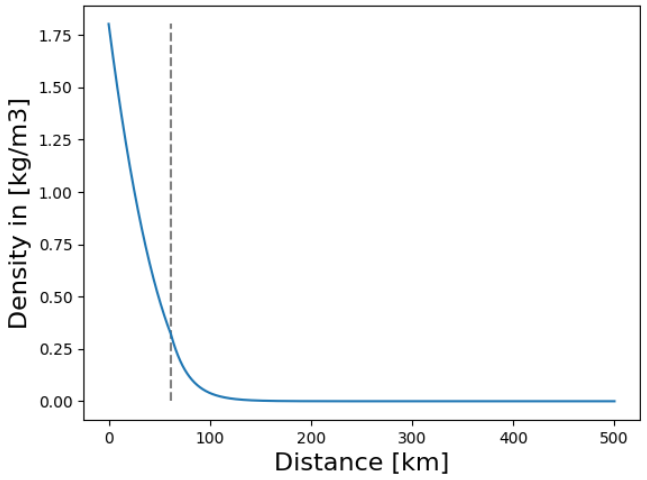

Figure 8. Density profile from surface to 80 km above surface. The dotted line is the border between the adiabatic and isothermal atmosphere at about 500km above the surface.

II. DISCUSSION

A. Low orbit

Low earth orbit is defined by an orbit with a period of no more than 128 minutes, and an eccentricity of no

more than 0.25 (2022). We are well within the requirements for eccentricity, but just outside for period time, as we need 134 minutes to complete an orbit. However, this is a very unfair comparison, because we are considering two different planets. The earth is much bigger and more massive than planet 1, meaning a bigger diameter and different gravitational pull. Still, if we defined low orbit for this planet, we would probably still not qualify, because we are not as close as we could get. The reason for this is that we did not know at what distance the atmosphere begun to affect the orbit, so we played it safe and only got as close as we had to for taking pictures of the surface.

B. Landing destination

The landing destination pictured in 4 was chosen as it seemed very practical. Seeming rather flat, especially to the left of the image, the spaceship would not have to move through much terrain while landing. Our spacecraft is currently moving clockwise around the planet, on the picture this is to the right. So during a landing we will hit the atmosphere and most likely drift a bit clockwise, also seen as to the left of the image, where it continues to be flat. Additionally the space to land is very big, meaning our landing would not have to be so exact and as it is on the day side it would let us see during landing. Therefore we decided that this is the perfect spot to begin landing.

C. χ^2-minimization

To find the best model to math the data we used the method of χ^2-minimization. This method is much like the least squares described in *Celestial mechanics* 2022. As a short reminder for the reader, the least squares method takes the difference between a measured value and an expected value, squares this value to ensure that it is positive, and then sums up this square with the square from all other data points. With χ^2-minimization, we do just that, but before squaring, we divide by the standard deviation in that point. This is so that points with a higher standard deviation, more noise, are less weighted. This makes for a better method as long as we know the standard deviation in each point, like we do here. This is especially applicable when we have noisy data, and when the noise varies, like in this case.

D. Gibbs inspired optimizer

When making a model for the line profile, we need three parameters, the wavelength in the middle of the profile λ, the temperature T, and the flux at the bottom of the line profile F_{min}. This simply means that in order to find the best model, we have to find the combination of these three parameters that fit best. To do that we utilize an algorithm inspired by the Gibbs sampling method. Refer to *"Explaining the Gibbs Sampler". The American Statistician. (1992)* for a complete description of the Gibbs sampler. The idea that we borrow is that of searching only one parameter, or one axis of the parameter-room at the time, and then use the most likely value when searching the next parameter. This means that we freeze two of the three parameters, and vary the last. With χ^2-minimization we can find the best fitting value for that parameter while the two other are frozen. Once we have that we use this new value, while we vary an other parameter and so on until the three parameters converge to their final values. These are the values we use for our final model.

This method has strengths and weaknesses. The main weakness is that this method does not consider all combinations of the three parameters. In other words, we do not search the whole parameter space. This means that this method might completely miss the real best model. Imagine we only have two parameters, so that our parameter space is a plane. Then let us represent χ^2 for each combination of the parameters as a scalar field in the parameter space. We know that the minimum in the scalar field is the best match, so this is the point we are trying to find. When using this algorithm and keeping one parameter constant, we then only search a line in the parameter space. Study figure 9 to see how these lines would look. We then find the lowest value on that line, meaning the most likely value, keep that value constant and draw a new line through that point. We repeat this pattern and draw a path through the parameter space until we converge in a point. The problem with this is that we can find situations like that in figure 9. Here the Gibbs sampling method converges in point A, and completely misses point B, even though B is the global minima, and therefore the parameters for the best model. This results in us completely missing the true best match.

A strength of this Gibbs sampler inspired method is the computation time. Since we only search different lines in the parameter space and not the whole space, we can get away with way fewer calculations. If we were to search the whole parameter space with a fully vectorized program, each absorption line you would be looking for would have you do operations on a four dimensional array. For the same grid resolution as we used for our results, these arrays would have roughly 100.000.000 elements compared to our two dimensional arrays with only 10.000 elements. This is assuming that we do all the same operations for χ^2-minimization and with the same grid resolution, which again means that the results will be equally precise provided our method converges in the correct minima. It is however true that we have to run several iterations in order to find the minima. We landed on 10 iterations, even though most of the spectral lines converged after only 5 iterations.

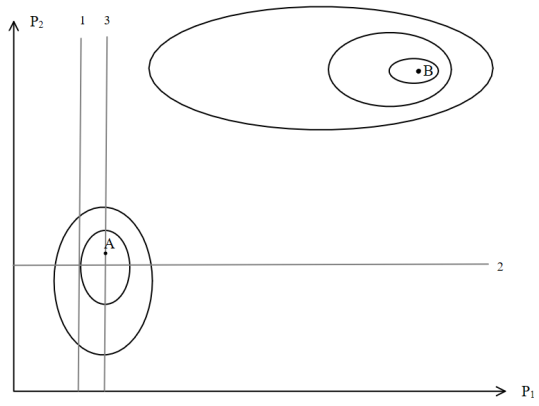

Figure 9. Each axis represents a parameter. A and B are two minima of the scalar field representing χ^2, where B is the global minima

E. Optimization

As we discussed earlier, a weakness of our method is that it might miss the global minima. One way of trying to lower the probability of converging in the wrong minima, is to have a good initial guess. For the case in this paper, a good guess for λ is the wavelength of that line if it were not shifted by the Doppler effect, (λ_0). We have no reason to assume that the spectrum is blue-shifted rather than red-shifted, or opposite. For this reason we should start guessing that there is no shift at all. For the temperature T we know that it is between 150K and 450K. We have no reason to think that the temperature is closer to the lowest or the highest value, so we just start in the middle. Finally, for F_{min} we know that it has a minimum possible value of 0.7, and that very small values of F_{min} means small profiles that are very likely to be lost in the noise anyways. For this reason we start at 0.7 to search for profiles that are easier to distinguish from the noise.

We must also consider how many values of each parameter we should search. Let us call the grid-resolution N. Having a many values can mean more precise results, but definitely means longer run-time. In order to decide N we, tested different values and found that going from $N = 100$ to $N = 1000$ only slightly improved the precision. We will come back to how precise our algorithm is with $N = 1000$ in II. D.. However, the run-time when iterating the Gibbs method 10 times went from 2.810 seconds with $N = 100$ to 10.34 seconds for $N = 1000$. Even though this is a significant increase in run-time, 10 seconds is still not very long, and an acceptable wait for even slightly better results.

We must also decide the number of iterations of the Gibbs sampler. We define one iteration as updating every parameter once. As stated earlier, we found that most of the spectral lines converged, meaning the updated value was the same as the previous, already after 5 iterations. We tested this simply by printing the values and observing when they stopped changing. In a future version we could design the algorithm to decide for it self when it converges and stop iterating after that. For 5 iterations with $N = 1000$ the algorithm runs in 6.186 seconds. Increasing the iterations to 10 in order to be sure that everything converges, only increases the run-time by 4.15 seconds. We consider this an acceptable sacrifice. However, if we had to search for more than the 12 absorption lines we are looking for now, one quick way to save time would be to decrease N and the number of iterations. This is not a big loss, because, as we will see soon, the models are not very precise anyways.

F. Testing the applied Gibbs method

In order to test this method, we constructed a line profile and distorted it with a Gaussian noise with the same standard deviation as the real data. This was so that the χ^2-minimization would still be applicable, and to really see how much the noise affects the data. We found that the relative error for T and F_{min} was way more than that for λ. First we looked at the random line profile with $\lambda_0 = 800$, $T = 355$, $F_{min} = 0.8$ moving with a relative velocity compared to the measuring instruments of 4.0×10^3 km/s. Then we fed the algorithms we used for finding the absorption lines with the distorted data. We do this with the goal of seeing how close our algorithm is to finding the original line we hid in the noise. We did this 50 times, because for each time we scrambled the line profile we get different versions of the data, and we needed to make up for the fact that some random scrambles produced way more precise results than others. After this process we took the mean relative error of each of the parameters needed to make a line profile. We got the following relative errors:

$$R_\lambda = 3.1 \times 10^{-6}$$
$$R_T = 0.41$$
$$R_{F_{min}} = 0.060$$

We see that the relative error for λ is much smaller than for the two other parameters. To make sense of this we looked at the produced graph of the curves individually and found that the models were often deeper and thinner than the real line profile. This is probably a byproduct of how the noise makes for dramatic spikes, and that the sampling frequency when collecting the data is not as high as one could hope for. This results in the algorithm favouring sharp curves, and T and F_{min} being less reliable than λ. It is also worth mentioning that the segments for longer wavelengths have more data points because of the way the segments are chosen. It is also worth mentioning that when physically looking through the graphs of 20 returned line profiles, 17 of

those had the model in the right "pit", while the 3 other were somewhere else completely. This tells us what we already know, that the Gibbs sampling either finds the right "pit" quickly and efficiently, or is completely wrong.

The relative error varied in different segments of the complete data as the standard deviation varied. Take for example the segment around 720nm where we can see from the graph in the appendix that there is little noise. The mean relative error when testing the line profile as described previously was the following:

$$\begin{aligned} R_\lambda &= 1.4 \times 10^{-7} \\ R_T &= 0.19 \\ R_{F_{min}} &= 0.025 \end{aligned}$$

Which is significantly less. We can also look at the segment around 630nm where the data is especially noisy as find, as expected, higher relative errors.

$$\begin{aligned} R_\lambda &= 5.5 \times 10^{-6} \\ R_T &= 0.42 \\ R_{F_{min}} &= 0.071 \end{aligned}$$

Knowledge of this helps us consider which absorption lines are real and which are flukes.

G. Separating the real from the flukes

When trying to separate the real absorption lines from the flukes, we have a few guidelines. For one, every absorption line should have the same shift. This is because the detector's relative speed to the atmosphere being analyzed is the same for all the gasses in the atmosphere. Secondly the spectral lines of a gas should share the same temperature. And lastly we have to evaluate how much noise we have in the segment we are looking at in order to evaluate how much we can trust the data we get.

Once the algorithms have done their job to find the best matching model, it is up to us to use our intuition to decide the final result. This also means that a lot of the evaluations done from this point on are based on educated guessing and gut-feeling. We see that almost all of the models are shifted to the right, which means that they are red-shifted. Now we can discard the two blue-shifted lines. We also know that real lines tend to have lower F_{min} values, so the less pronounced "pits" can be discarded. This leaves 6 spectral lines to be considered. These are the following: O_2 690nm, H_2O 720nm, H_2O 940nm and CO 2340nm. Of these, the two H_2O lines look very good, and have approximately the same temperature, which is a good sign. The 720nm spectre even has relatively little noise, which strengthen its case even more, supporting the other H_2O line as well. H_2O has one more spectral line at 820nm, that could be a real one, but it is not very pronounced. However both its shift and temperature match the other two pretty well. Next O_2 690nm looks reasonable, and has matching shift to the other two, however the associated segment is noisy, the other two O_2 lines have little to support them. We will still consider it probable. Lastly CO 2340nm looks very good and gives me a good gut-feeling, however its shift is significantly larger than that of the trusted H_2O lines. While the H_2O lines had a shift of 0.2nm, CO has a shift of 0.5nm. However, the CO-segment is particularly noise-free, this leads us to include it against our better judgement.

H. Forward Euler for solving ODEs

To calculate density and temperature we had to solve a differential equation for pressure which we solve using Forward-Euler method. This gave us

$$P_{n+1} = P_n - dr\rho_n g_n$$

With ρ being the density at a given point and g_n the gravitational acceleration. dr is the step, in this case in m between the calculations.

As this is a numerical approximation, meaning all numbers are prone to an error. The higher amounts of step, so the lower the actual value of the step, the more accurate the calculations becomes. The step we settled for needed to be high enough to no longer have an substantial error, but it also needed to be computale.

To measure this, we computed with different time steps and measured the relative error between the final density values. As seen in table I, there is a minuscule difference between 0.01 and 0.001 of about $4.487 \cdot 10^{-6}$%. The fault decreases by 10% for a 10 times lower step. Because there is only such a small scale error between 0.01 and 0.001 we determined the results with a step of 0.01 to be satisfactory.

dr	Fault
0.1	$4.487 \cdot 10^{-5}$%
0.01	$4.487 \cdot 10^{-6}$%

Table I. The relative error to a 10 times lower step (dr). The difference between the step 1 and 0.1 is $04.487 \cdot 10^{-5}$%. The difference between step 0.01 and 0.001 is $4.487 \cdot 10^{-6}$%.

I. Measures for atmospheric profile

To produce our atmospheric profiles we assumed that the atmosphere is in a state of hydrostatic equilibrium, meaning it is stable, as the gravitational force is perfectly counteracted by the pressure forces. We are working with a light weight planet with weight of $1.684 \cdot 10^{-5} M_\odot$, which lighter than mercury. Yet, as it also smaller than mercury, it is not at high risk of lacking enough gravitational

forces to hold an atmosphere stable. With a radius of about 2404 km, we can assume that the condition for hydrostatic equilibrium is still fulfilled. Another way of looking at it is that our planet is twice as big as Pluto, yet ways 20 times as much. So we are not at risk of working with a dwarf planet, a planet lacking not in hydrostatic equilibrium, therefore lacking an atmosphere.

Another question was how far the atmosphere goes on for. We could measure until the density or pressure solved was nearly identical to the density or pressure in space. However as space nears a vacuum, both values would be incredibly small. According to Vacuum Technology, (2012) A. Roth, a satisfactory vacuum has a pressure around 19 orders of magnitude smaller than on earths surface. To reach such a number would take ages. Also with such small values the error from the Forward-Euler method might cause issues. Even for the earth there is no clear line where the atmosphere stops. Instead there has been set the boundary with the Kármán line at 100 km above the earths surface.

Instead of finding where the atmosphere could stop we instead looked at it relative to the spacecraft. As the low orbit was not effected by the atmosphere at a height of 500km we just set the boundary there. As our profile can be calculate at what ever height it was no issue to move the boundary around.

J. Analyzing of the atmospheric profile

Further we wanted to analyze if our results seemed realistic, so we compared our atmospheric profile with mostly that of Earth and somewhat to Venus and Mars to gauge the results. In doing so we expanded our view on if the planet is livable at surface level. The Earths and other planets values are much more complicated, yet still roughly comparable. They obviously do not follow the simplifications we have. Refer to International Civil Aviation Organization. Manual of the ICAO Standard Atmosphere for values on earths atmosphere.

In figure 10 we see an overview of the relative decline of pressure, density and temperature from the surface to the distance of 500 km. It gives a nice overview of how the different quantities behave over the height atmosphere.

First we look at the temperatures behaviour. The linear decrease in the adiabatic atmosphere is expected. It mirrors the temperatures behaviour in the earths troposphere, which is not far from adiabatic. When it reaches the isothermal model, it acts similar to earths Tropopause, which also borders to be isothermal. Unlike earth, the temperature drops over much longer distance, with the isothermal phase only starting at 61.65km. Comparatively the tropopause is only between 12 to 18 km above the surface. We modeled the temperature in the atmosphere as constant after 61.km. In comparison the earths atmosphere sees extreme changes due to different atmospheric effects we neglected.

In figure 11 we have the profile of the pressure from the

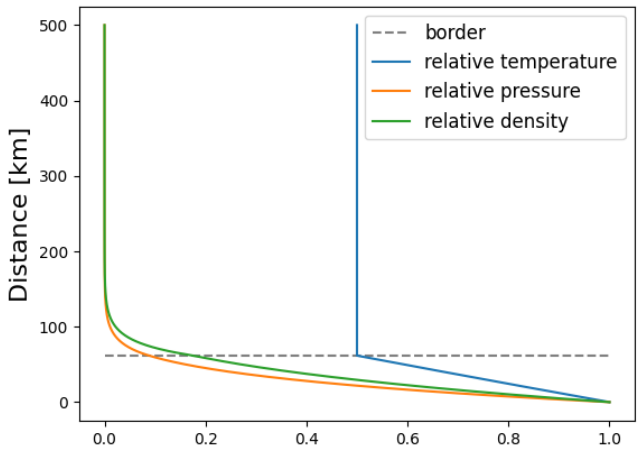

Figure 10. The relative decline of density, temperature and pressure against distance from the surface in km on the y axis. The dotted line is the border between adiabatic and isothermal atmospheres

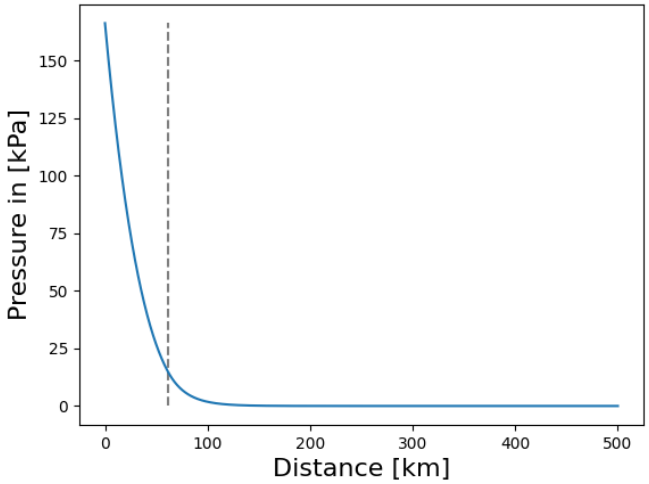

Figure 11. Density in kPa from 0 to 500 km above planet surface. The dotted line is the border between adiabatic and isothermal atmospheres

surface to 500km. This is a byproduct of the computations for temperature and density. It starts at $166.3kPa$ or $1.663bar$. $1bar$ nearly equates to earths atmospheric pressure at sea level. So essentially the surface pressure is 1.6 times stronger than on earth. With a higher starting density and similar temperature this result is expected.

The pressure drops quite slowly, as it only reaches about half the original pressure at $43586km$ while on earth it already reaches this at 5.5 km altitude. The pressure ends at a value of $1.657 \cdot 10^{-5} Pa$

We start with a density of about $1.802 \frac{kg}{m^3}$, which drops quite slowly to begin with, but nears 0 in the end. This is logical as the pressure falls the gasses in the atmosphere become less dense, as less force is compressing them. At the transition from adiabatic to isothermal

the density begins to shrink quicker. In comparison is there no change in the pressures exponential recession rate when shifting from adiabatic to isothermal as seen in figure 11. This is also evident in the analytical formula for atmospheric pressure 1. Therefore the increase in densities decrease is because the temperature is now constant, meaning the drop in pressure is now only caused by a drop in density.

In general it seems that planet-1s atmosphere stretches out much further than earths. Yet as we made many simplifications we do not know to what extent this is true. For example our atmosphere is modelled as evenly distributed and at higher altitudes we did not incorporate more complicated aspects of atmospheric dynamics.

III. CONCLUSION

We successfully entered a circular orbit close enough to scout the surface for landing sites. We have not entered the atmosphere and can safely coast until we are ready for landing.

We used this low orbit to take multiple pictures of the planet while coasting around it and determined a landing site

We found that χ^2-minimization and Gibbs sampling are sufficient methods of finding spectral lines in quite noisy data, as long as you can make an educated evaluation of the computational results. Doing this we found that this atmosphere is mainly composed of water vapor, oxygen and carbon monoxide.

With this we found the mean weight of the atmosphere. Following some simplifications we could produce a profile of the temperature, density and pressure in the atmosphere. We found that the adiabatic part of the planets atmosphere has a height of 61.km.

IV. REFERENCES

Candidate 15342, Candidate 15341, (2022) *Celestial Mechanics*

Casella, G.; George, E. I. (1992). *"Explaining the Gibbs Sampler". The American Statistician.*

Definition of low orbit https://en.wikipedia.org/wiki/Low_Earth_orbit, 11.11.2022, retrieved 28.11.2022

International Civil Aviation Organization, (1993) *Manual of the ICAO Standard Atmosphere*

Vacuum Technology, (2012) A. Roth

V. APPENDIX

A. The absorption spectre

Read this before looking at the graphs in this section, they will make way more sense.

The following graphs are segments of a complete data set of flux measurements from wavelengths 600 nm to 3000 nm. In this case we have an absorption spectre where the Data has been normalized so that no absorption would give a flux of 1. Each figure is a segment of this absorption spectre. Each segment is centered around a possible absorption line as if it were not shifted by the Doppler effect. However the line might be shifted. We have assumed that our relative speed to the gas we are analyzing is no more than 10 km/s, and so the segment includes only the interval of wavelengths possible for each absorption line.

The blue curve is the data, and the orange is the best model. As you can see, the data is subject to a lot of noise, but not every segment of the absorption spectre is equally noisy. You can get a good idea of this by checking how far the spikes reach above 1 on the flux-axis. We know that the real spectre should not surpass 1, and so all of this must be noise.

B. Analytical pressure

$$P_h = P_0 e^{\frac{-\mu g h}{kT}} \tag{1}$$

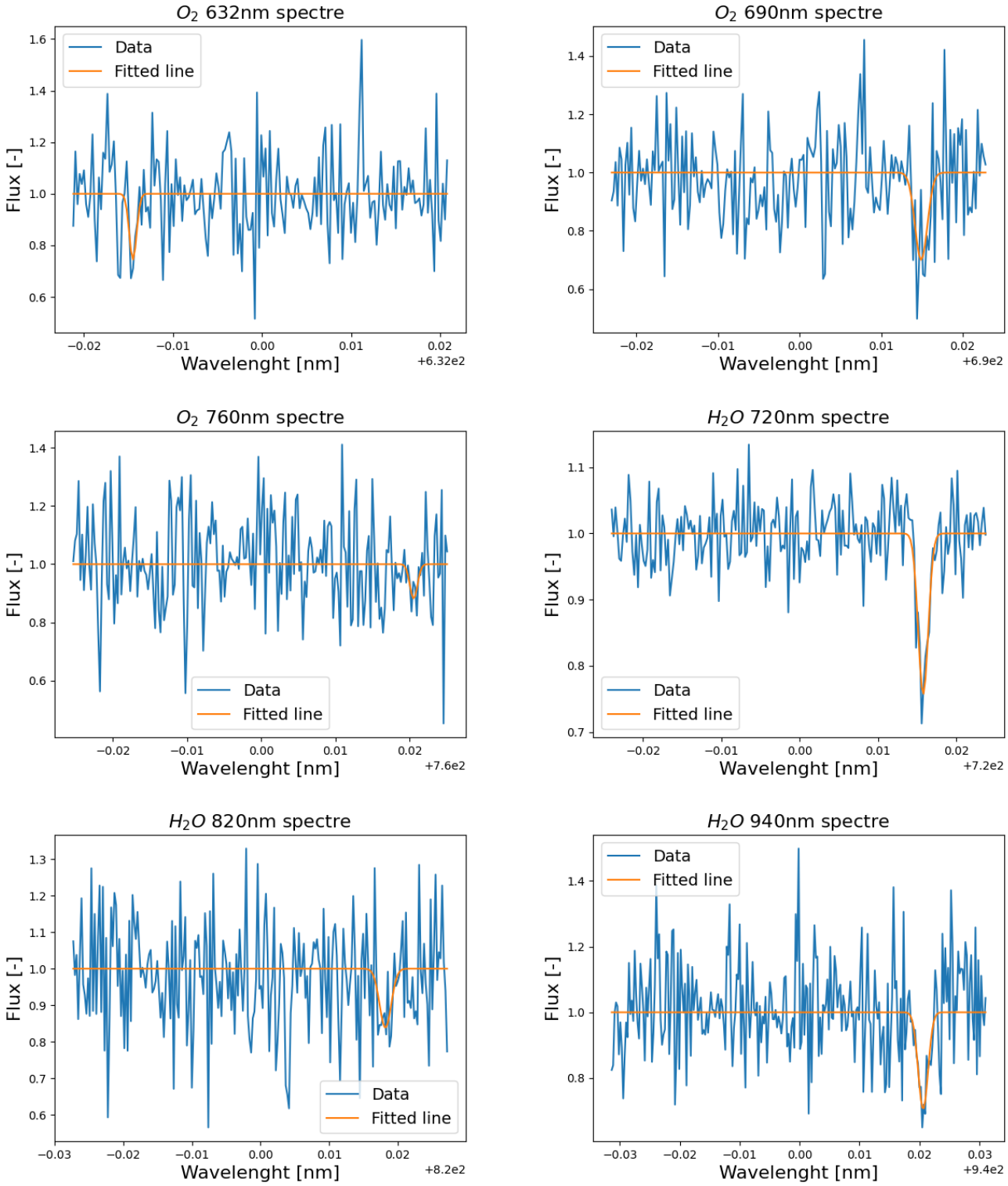

Figure 12. Blue graphs represent normalized flux-measurements of atmosphere. Orange line is a fitted Gaussian line profile of an absorption line. Fitted using χ^2-minimization over three parameters.

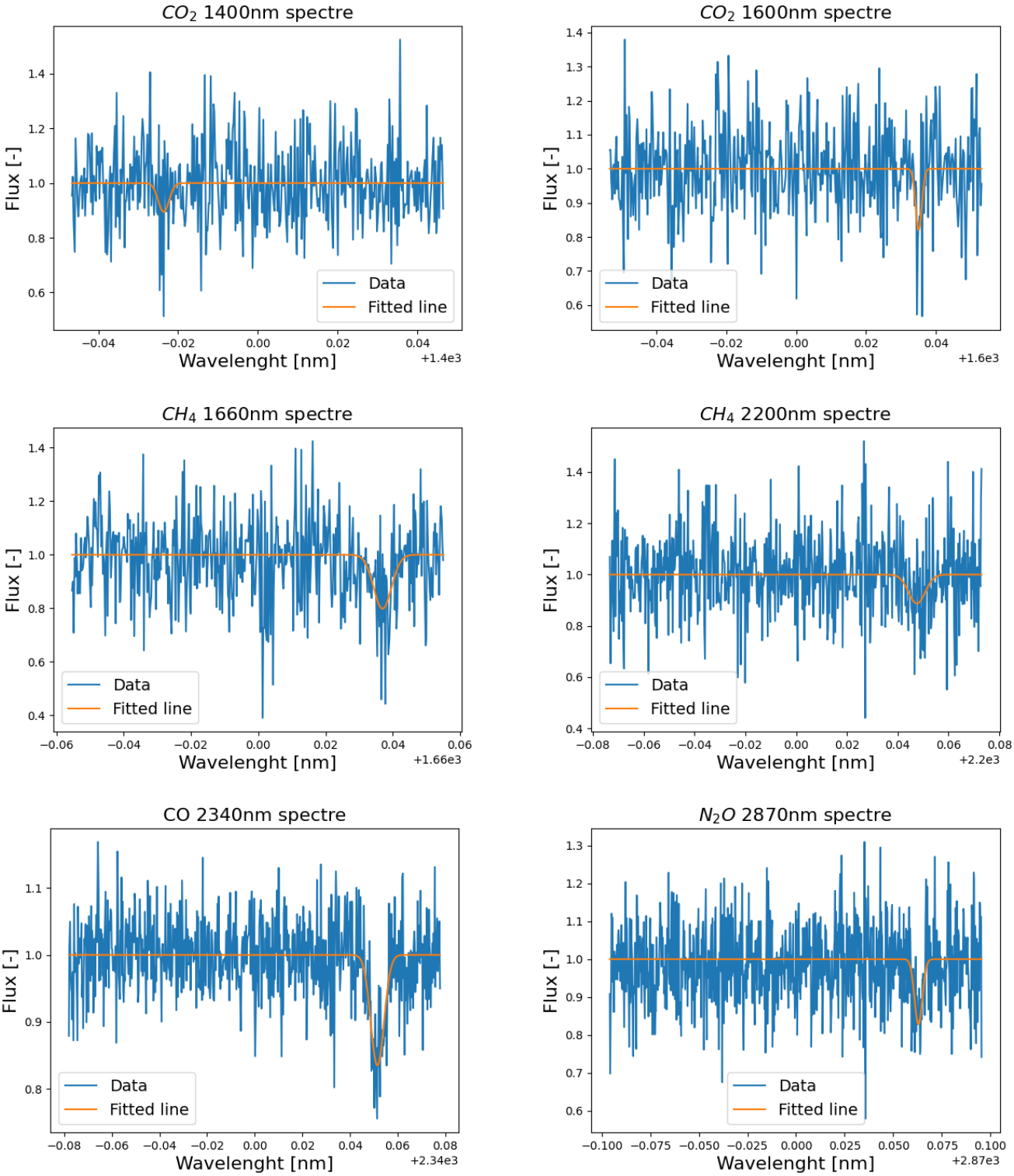

Figure 13. Continuation of figure 8